Dalton Transactions

Investigating subtle 4f vs. 5f coordination differences using kinetically inert Eu(III), Tb(III), and Cm(III) complexes of a coumarin-appended 1,4,7,10-Tetraazacyclododecane-1,4,7-triacetate (DO3A) ligand

Journal:	*Dalton Transactions*
Manuscript ID	DT-ART-04-2018-001547
Article Type:	Paper
Date Submitted by the Author:	26-Oct-2017
Complete List of Authors:	Junker, Anne Kathrine ; University of Copenhagen, Nano-Science Center & Department of Chemistry Deblonde, Gauthier; Lawrence Berkeley National Laboratory, Chemical Sciences; E O Lawrence Berkeley National Laboratory, Abergel, Rebecca; Lawrence Berkeley National Laboratory, Chemical Sciences Sørensen, Thomas; University of Copenhagen, Nano-Science Center & Department of Chemistry

Journal Name

ARTICLE

Investigating subtle 4*f* vs. 5*f* coordination differences using kinetically inert Eu(III), Tb(III), and Cm(III) complexes of a coumarin-appended 1,4,7,10-Tetraazacyclododecane-1,4,7-triacetate (DO3A) ligand

Received 00th January 20xx,
Accepted 00th January 20xx

DOI: 10.1039/x0xx00000x

www.rsc.org/

Anne Kathrine R. Junker,[a] Gauthier J.-P. Deblonde,[b] Rebecca J. Abergel[b]* and Thomas Just Sørensen[a]*

In order to reveal subtle differences between the solution chemistries of trivalent 4*f* and 5*f* elements, the physicochemical and photophysical properties of europium(III), terbium(III) and curium(III) complexes formed with a 7-methoxy-coumarin appended 1,4,7,10-tetraazadodecane-1,4,7-triacid (DO3A) ligand were studied. All three complexes were found to be kinetically inert and exhibit stability constants similar to their 1,4,7,10-tetraazacyclododecane-1,4,7,10-tetraacetic acid (DOTA) equivalents. The Cm(III) and Eu(III) complexes feature strong sensitised emission, while the triplet energy of the coumarin prohibits efficient sensitisation of the Tb(III) analogue. The data presented here indicate significant differences in perturbation of the sensitising chromophore photophysics between the 4*f* and 5*f* elements. In contrast, the size of the metal center appears to not be a determining factor for the physicochemical properties of these kinetically inert Eu(III), Tb(III,) and Cm(III) complexes.

Introduction

Our understanding of the solution chemistry of lanthanide(III) ions has vastly expanded over the last three decades,[1-4] through a research surge primarily driven by three key applications: i) Gd(III)-based MRI contrast agents,[5-9] ii) extremely sensitive bioassays exploiting Eu(III) and Tb(III) centred luminescence,[6, 10-13] and iii) the separation sciences essential to supplying pure lanthanide compounds for industrial applications.[14-16] One outcome of this research is that we now have the tools to probe and control the structure and speciation of lanthanide(III) ions in aqueous media,[17-20] in particular when working with kinetically inert complexes. This new level of control informs the design of responsive luminescent probes,[21-26] and allows for detailed physico-chemical investigations in solution.[19, 27-32] Extensive published work has determined that ligands comprising a cyclen scaffold and three or four carboxylate (e.g. DO3A, DOTA…) or carboxamide (e.g. DOTMA) pendant arms are heptadentate and octadentate, respectively, when complexing *f*-element ions.[1, 3] Furthermore, numerous studies have established paramagnetic ^{1}H NMR, time-resolved luminescence, and the Horrocks' equation as reliable tools for probing the coordination environment of lanthanide ions upon binding to such chelators.[3, 18, 19, 33-35] With these tools well-suited for the 4*f* elements in hand, the natural next step is to use them to investigate the solution chemistry of the 5*f* elements, albeit such development has been hampered by the radioactive nature and low availability of the actinide isotopes.

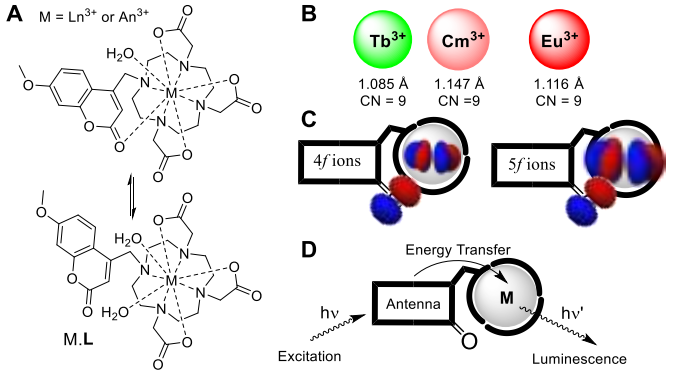

Figure 1. Molecular structure of the investigated complexes M.**L** and the equilibrium between a hepta- and octadentate binding mode (**A**), a scaled representation of the ionic radius of Eu(III), Tb(III), and Cm(III) ions (**B**),[36] an illustration of the difference in radial expansion 4*f* (inside ionic radius) and 5*f* (extends beyond ionic radius) orbitals (**C**), and a schematic representation of the antenna principle (**D**).

Contrasting the chemistry of 4*f* and 5*f* elements in aqueous solution is particularly relevant to elaborate on the behaviour and speciation of the latter man-made elements, for which the lanthanides have traditionally served as model systems. Although other oxidations states have been observed and are accessible in aqueous environments for the heavier

[a] *Nano-Science Center & Department of Chemistry, University of Copenhagen, Universitetsparken 5, 2100 København Ø, Denmark. E-mail: TJS@chem.ku.dk*
[b] *Chemical Sciences Division, Lawrence Berkeley National Laboratory, Berkeley, California 94720, USA. E-mail: rjabergel@lbl.gov*
Electronic Supplementary Information (ESI) available: synthetic protocols and characterisation, all optical spectra, details of quantum yield determination, time-resolved luminescence decay profiles, and spectrofluorometric competition batch titrations are included as ESI. See DOI: 10.1039/x0xx00000x

transplutonium elements, comparisons involving lanthanide ions are often limited to the trivalent state. In addition, while recent reports include series of complexes of heavy actinide ions with dipicolinate and hydroxypyridinonate ligands,[37-40] few kinetically inert complexes have been reported.[41-43] Here, we investigate a series of kinetically inert complexes of Eu(III), Tb(III), and Cm(III) to decipher subtle coordination differences between the 4*f* and 5*f* elements, using a macrocyclic ligand appended with an antenna chromophore (**L**, Figure 1).

In the actinide series, Cm is a paradigm for direct comparisons with Tb(III) and Eu(III) since (i) it has long-lived isotopes (e.g. ^{248}Cm, $t_{½}$ = 340,000 yr) that can be produced and purified on the multi-gram scale, (ii) in aqueous solution it is exclusively found in the +III oxidation state and, (iii) trivalent Cm(III) can readily be sensitised by organic ligands in aqueous media.[40, 42-51] The three metal ions probed in this study, Eu(III), Tb(III), and Cm(III), are very similar in size, as indicated by their respective ionic radii (Fig. 1, Δr = 0.03 Å), and, from a coordination chemistry perspective, can almost exclusively be differentiated by the nature of their valence electrons. For Cm(III), with electrons in the 5*f* shell, orbital overlap between metal- and ligand-centred orbitals is possible. This is not the case for the lanthanide(III) ions.[52-54] This feature is the main contributor to the differences in coordination chemistry or in the photophysical properties observed when contrasting antenna-appended complexes of 4*f* and 5*f* elements.

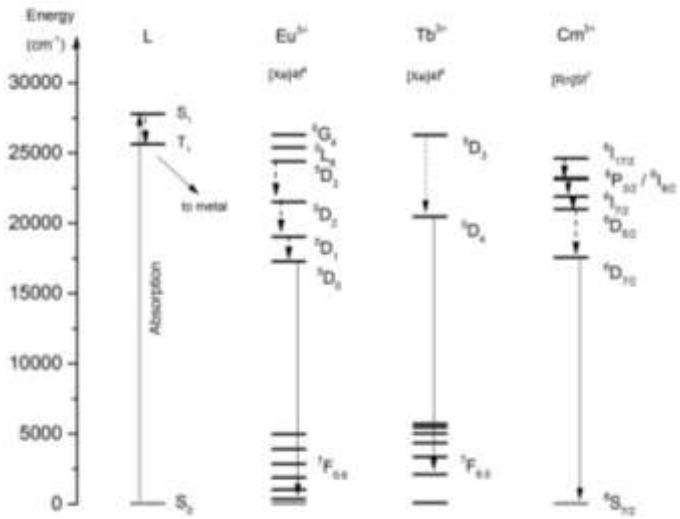

Figure 2. Energy levels of the coumarin antenna chromophore (**L**) and the Eu(III), Tb(III), and Cm(III) free ions.[55, 56]

As depicted in Figure 1, we chose for this work the 7-methoxy-coumarin appended DO3A ligand (**L**), which can be either hepta- or octadentate, depending on whether the coumarin moiety coordinates the central metal ion or not.[1, 23, 25, 57] For sensitised *f*-element luminescence, the convention is that excitation into the antenna singlet excited state manifold is followed by rapid inter-system crossing to the triplet excited state manifold. For the 7-methoxy-coumarin antenna, only the first excited singlet state and the lowest lying triplet state are relevant under the experimental conditions used in this study. Figure 2 shows the relevant metal-centred excited states for Eu(III), Tb(III), and Cm(III). Cursory inspection reveals that the three *f*-elements can be sensitised by the coumarin, and that the energy gap between the coumarin triplet state and the metal-centred state at >4,500 cm^{-1} should give rise to irreversible population of the metal-centred emitting states.[21] Thus, this system was deemed ideal for contrasting the photophysics of antenna-appended complexes of a 4*f* and a 5*f* ion.

Results and Discussion

Synthesis

The ligand was synthesised in two steps from readily available starting materials as shown in scheme 1. The first step consists of an alkylation reaction between the hydrobromide salt of tris(*tert*-butyl ester) substituted DO3A[58] and 4-bromomethyl-7-methoxy-coumarin using standard alkylation conditions that is potassium carbonate and acetonitrile heated to 60°C overnight. The resulting preligand (**1**) was purified by column chromatography on silica gel to afford the protected ligand or pre-ligand as an off-white solid in 45% yield. In a second synthetic step the triester precursor was then converted to its triacid form by treatment with a 1:1 mixture by volume of trifluoroacetic acid and dichloromethane. The deprotection was completed by stirring the reaction at room temperature for 48 hours. Repeated trituration with diethyl ether from methanol yielded quantitative amounts of the ligand (**L**), isolated as an off-white solid in a quantitative yield. Both preligand (**1**) and ligand (**L**) were characterised by ^{1}H and ^{13}C NMR spectroscopy and high-resolution mass spectrometry. The complexes (1.68 µM) were assembled *in situ* from stock solutions by mixing 1:1 equivalent of ligand (**L**) and metal ions in aqueous HEPES Buffer (pH 7.4).

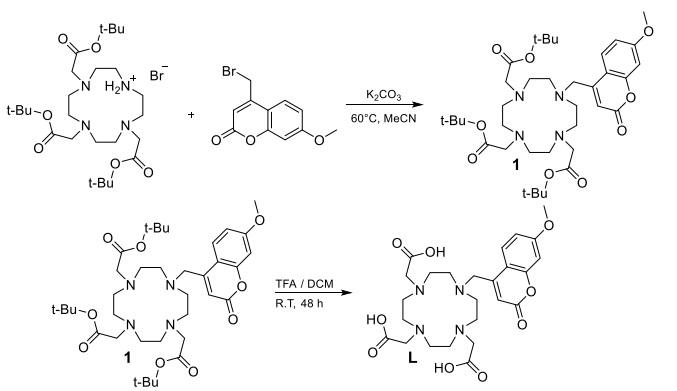

Scheme 1. Synthetic pathway to **L.**

Luminescent properties

The luminescence properties of the complexes were probed using steady-state and time-resolved emission spectroscopy. The ligand-centred emission, fluorescence from the coumarin-centred first excited singlet state, is modulated by the presence of the *f*-elements. With Eu(III), the coumarin fluorescence is significantly quenched and the observed fluorescence quantum yield (ϕ^{Eu}_{fl}) is reduced from 22 % for the free ligand to 7 % for the complex. The coumarin fluorescence intensity is reduced to

ϕ^{Tb}_{fl} = 18 % in the Tb(III) complex, while it remains unperturbed upon Cm(III) binding, with ϕ^{Cm}_{fl} = 21 % (Figure 3 and Table 1). The transition energy is redshifted to 412 nm in the Cm(III) complex from 407 nm in the Eu(III) and Tb(III) complexes. This difference clearly indicates mixing of the 5*f* orbitals and the π-system of the antenna chromophore, as i) it is the only difference between the 4*f* and 5*f* complexes, and ii) mixing of states would result in a change of the transition energy without a change in the excited state processes depopulating the singlet state located in the π-system.

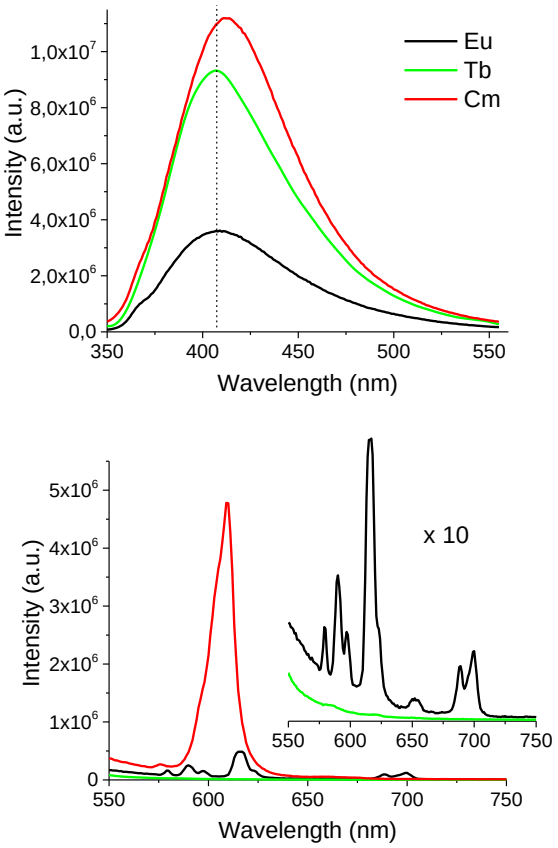

Figure 3. Ligand centred fluorescence (top) and metal centred emission (bottom) following excitation at 325 nm. The data are directly comparable as the data were recorded with identical settings and the same metal and ligand concentrations (1.68 µM) in HEPES buffer at pH 7.4.

In contrast, Eu(III) significantly promotes non-radiative deactivation. While photoinduced electron transfer (PeT) is only possible for Eu(III),[59] the heavy atom promoted inter-system crossing is expected to be similar for all three ions. Thus, the reduced fluorescence intensity in the Tb(III) complex suggests sensitisation of the lanthanide centred-excited state by the singlet state of the antenna. Figure 3 shows the metal-centred luminescence for the three complexes upon excitation into the chromophore first excited singlet state. The excitation spectra (see ESI) show no sign of metal-centred transitions, which suggests that the luminescence is dominated by sensitised emission *i.e.* the antenna-centred excited state is the origin of the metal-centred excited state. For Eu(III) and Cm(III), the 7-methoxy-coumarin is an efficient sensitiser, whereas only a very weak Tb(III) centred emission is observed. The latter must be due to a poor overlap of the antenna excited states with Tb(III) centred excited states. The ligand-centred triplet state is too high in energy for the excited state energy transfer to be reversible (Figure 2), a fact that is supported by the time-resolved data. In the Eu(III) and Cm(III) complexes, the excited state energy transfer from the antenna-centred triplet donor state is possible for several metal-centred acceptor states (Figure 2). The strict requirements of the Dexter energy transfer mechanism operating for the 4*f* ions, may be relaxed by mixing indicated by the redshifted emission spectrum of the antenna in the case of the 5*f* Cm(III) ion.

Table 1. Selected physicochemical properties of the metal ions, binding constant of the investigated ligand system **M.L** contrasted to selected polyaminocarboxylate ligands, and photophysical data for metal- and ligand-centred emission for complexes of europium(III), terbium(III) and curium(III).

	Eu	**Tb**	**Cm**
Ionic radius (Å)	1.116[36]	1.085[36]	1.147[36]
M.L Log β^{a*}	27.0 ± 0.2	29.0 ± 0.1	28.0 ± 0.5
M.DTPA Log $\beta^{a,b}$	22.91[60]	23.21[60]	22.99[61]
M.EDTA Log $\beta^{a,b}$	17.35[60]	17.93[60]	18.45[62]
M.DOTA Log β^{a}	23.7[63]	23.5[63]	-
M.DOTA Log β^{c}	23.95±0.11[42]	-	24.02±0.10[42]
M.DOTA Log β^{d}	28.2[64]	28.6[64]	-
Hydration energy[65] (kJ/mol)	3501	3559	3513
λ_{abs} (nm)*	329 ± 1	328 ± 1	327 ± 1
λ_{em}(nm)*	407 ± 1	407 ± 1	412 ± 1
ε (M^{-1} cm^{-1})*	3300± 300	3600 ± 400	3900 ± 400
log ε ($M^{-1}cm^{-1}$)*	3.52 ± 0.03	3.56 ± 0.04	3.59 ± 0.04
τ_{H2O} (ms)*	0.41 ± 0.001	0.91 ± 0.2	0.40
τ_{D2O} (ms)*	1.63 ± 0.003	1.2 ± 0.001	0.51
q (Horrocks)[e*]	1.9 ± 0.3	1.0 ± 0.3	-
n_{H2O} (Kimura)[f*]	-	-	0.7 ± 0.5
Ln or An ϕ_{Lm} (%)*	5.3 ± 0.5	-	11.8 ± 1.2
Coumarin ϕ_{fl} (%)*	7.3 ± 0.7	18.2 ± 1.8	21.4 ± 2.1
E_S (cm^{-1})*	26,700	26,700	26,700
E_T (cm^{-1})*	25,000	25,000	-

[a] 0.1 M KCl, 25°C, [b] 0.1 M NH_4ClO_4, 25°C, [c] –log*K* for the equilibrium: $M^{3+} + H_2O = M(OH)^{2+} + H^+$, 0.1 M $NaClO_4$, 25°C, [d] 1 M NaCl, 20°C. [e] equations $q = A(\tau_{H2O}^{-1} - \tau_{D2O}^{-1} - B)$, for europium(III) *A* = 1.2 ms and *B* = 0.25 ms, for terbium(III) *A* = 5.0 ms and *B* = 0.06 ms .[17, 18] [f] For Cm: $n_{H2O} = 6.12 \cdot 10^{-4} \tau^{-1} - 0.48$.[66] * This work.

Time-resolved data is instrumental to determine the average number of solvent molecules bound to the emitting metal centres (*q*). For the 4*f* ions, we used the modified Horrocks' equation,[18] while for the 5*f* elements we have to rely on Kimura's approach to determine the number of coordination water molecules or *n*.[45, 67] The experimentally determined coordination numbers are compiled in Table 1 and highlight the different behaviour observed for the Eu(III) complex. Only one first-coordination-sphere water molecule is observed for both Tb(III) and Cm(III), indicating that the ligand is binding those metals in an octadentate fashion, whereas the Eu(III) complex incorporates two water molecules, which could only occur with a heptadentate coordination mode. This difference in ligand

binding mode (octa- vs. heptadentate) may explain the weaker binding affinity for the ligand towards Eu(III), as detailed below.

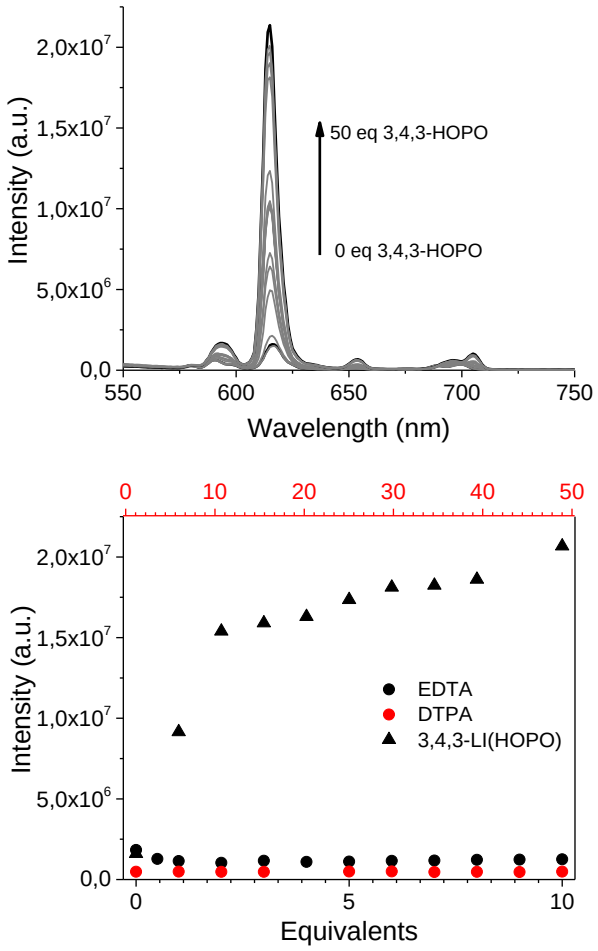

Figure 4. Top: Spectrofluorimetric competition titration of Eu.**L**. against 3,4,3-LI(HOPO) ([Eu.**L**] = 1.4 µM, [HOPO] from 0 to 70 µM, KCl 0.1 M, 10 mM HEPES, pH 7.4, 25 °C, exc = 325 nm). Bottom: change in emission intensity at 617 nm as a function of equivalents of competitor (EDTA, DTPA, and 3,4,3-LI(HOPO)) added.

Complex stability

The stability constants of the complexes were determined by competitive binding titration experiments, taking advantage of the metal-centred luminescence. First attempts using DTPA or EDTA as the competing ligand (up to 500 equivalents) did not result in any observable spectral change, highlighting the robustness of the DO3A-coumarin complexes. As a stronger competing ligand was needed, series of experiments were conducted using 3,4,3-LI(1,2-HOPO); a synthetic chelator whose solution thermodynamics with Eu(III), Tb(III), and Cm(III) were previously characterized and reported in the literature.[68-70] Upon addition of a 2-fold excess of 3,4,3-LI(1,2-HOPO), treatment at 60°C for four days, and 25°C for three days, the three DO3A-coumarin complexes could finally be challenged. In subsequent competition titrations, solutions containing an equimolar ratio of metal and DO3A-coumarin ligand ([M(III)] = [L] = 1.4 µM, [KCl] = 0.1 M, [HEPES] = 0.1 M, pH 7.4, 25 °C) were divided into separate aliquots and the competing 3,4,3-LI(1,2-HOPO) ligand were added to reach concentrations varying from 0 to 15 µM. The solutions were heated, allowed to reach equilibrium (when luminescence change was no longer observed) and an emission spectrum was recorded following excitation at 325 nm for each solution. The intensity change of the metal-centred emission upon addition of 3,4,3-LI(1,2-HOPO) corresponds to the formation of the new complex (see Figure 4). The data consisting of sets of emission spectra (λ_{em} = 550–750 nm) from solutions with varying concentrations of the competing ligand were imported into the refinement program HypSpec and analysed by nonlinear least-squares refinements.[71] The equilibration of the metal between both ligands was calculated by including the proton association of both ligands, the 3,4,3-LI(1,2-HOPO) complex formation constants, and the hydrolysis constants of the metals, as fixed parameters in the refinements and assuming that the emission intensity results exclusively from the sensitisation of the metal ion by the ligands. Each experiment was performed in duplicates. The resulting complex formation constants are compiled in Table 1, along with literature values for Eu(III), Tb(III), and Cm(III) binding constants with selected comparable ligands. Overall the stability of these DO3A-coumarin complexes is relatively high (log β > 27), indicating that the ligand binds all three ions strongly and forms kinetically inert complexes, as suggested by the remarkably slow ligand-competition assays.

Literature values for macrocyclic complexes are not fully consistent with each other, e.g. the stability constants (β) for [EuDOTA]$^-$ and [TbDOTA]$^-$ have been reported in both the 10^{28} and 10^{24} ranges.[42, 63, 64] Nonetheless, when using the same ligand within a given study, similar binding constants for the Eu(III), Tb(III), and Cm(III) complexes are found (Table 1). In contrast, the DO3A-coumarin complexes studied here exhibit different stability constants with the different metal ions. The log β values associated with Eu(III) and Tb(III) binding follow a trend expected with regards to the contraction of lanthanide ions, however a 2-order-of-magnitude difference between neighbouring lanthanides for a carboxylate-based ligand is unexpected and noteworthy (Table 1). The corresponding stability constant determined for Cm(III) is higher than expected, based on the size of the metal ion, its acidity and hydration energy (Table 1). Evidently, the coumarin pendant arm modulates the affinity of the DO3A binding pocket, disfavouring the larger Eu(III) ion and favouring the smaller Tb(III) ion. The affinity of the even larger Cm(III) ion lies between the two, possibly due to the involvement of the 5*f* orbitals in bonding.

Conclusions

In summary, we have reported the first antenna-appended DO3A complex of a 5*f* element. We have determined that the ligand forms kinetically inert complexes with Eu(III), Tb(III) and Cm(III), with a variation in complex stability that goes beyond simple electrostatic interactions and simple ionic radius trends. Further, the 7-methoxy-coumarin chromophore is an efficient

antenna for Eu(III) and Cm(III) centred emission with a high quantum yield of metal-centred luminescence (5.3% and 11.8%, respectively), while being a remarkably poor sensitiser for Tb(III). The Eu(III) centred luminescence quantum yield is particularly remarkable, as the Eu(III) centre has an average hydration number of 2. In this series of three complexes, the Eu(III) ion stands out with a different mode of coordination and a weaker binding constant. While the ionic radii of Eu(III) and Cm(III) are more similar, the physicochemical properties of Cm(III) complex resembles those of the Tb(III) complex. This stands apart from our general assumption that the ionic radius governs the coordination chemistry of the *f*-elements.

Experimental

All chemicals for synthesis were used as received. All solvents for spectroscopic experiments were of HPLC grade and used as received. Water was deionized and microfiltered using a Milli-Q Millipore machine. Chromatographic purification was performed on silica gel (SiO_2) with pore size of 60 Å and particle size of 60–200 µm. Mass spectra were recorded on a high resolution MicrOTOF-QII-system using ESP (calibrated using formic acid) HMRS mass spectra are included in the ESI Figures S3, S6, S7, and S8. ^{1}H NMR spectra were recorded on a Bruker 500 MHz instrument. ^{13}C NMR spectra were recorded on a Bruker 126 MHz instrument equipped with a (noninverse) cryoprobe. All chemical shifts (δ) are given in parts per million. ^{1}H and ^{13}C NMR spectra are included in the ESI Figures S1, S2, S4, and S5. The complexes presented in this report was prepared *in situ*, characterization of the isolated complexes can be found in reference 72.

Synthesis

1-(7-methoxy-4-methyl-coumarin)-4-7-10--tris(tert-butoxycarbonylmethyl)-1,4,7,10-tetraazacyclododacane (1). 4-Bromomethyl-7-methoxy-coumarin (546.7 mg, 2.03 mmol) was dissolved in acetonitrile (30 ml) together with 1,4,7-Tris(tert-butylcarbonylmethyl)-1,4,7,10-tetracyclododacane (1.10 g, 1.85 mmol) and potassium carbonate (1.15 g, 8.31 mmol), the mixture was heated to 60°C and stirred overnight. After the reaction was complete the mixture was filtered and washed with dichloromethane. The filtrate was then evaporated to dryness under reduced vacuum. The crude product was purified by column chromatography (10 % MeOH/DCM). Yield 586 mg, 45%. ESI-MS: m/z calculated for $C_{37}H_{58}N_4O_9$ $[M+H]^+$ 703.4276, found 703.4287. ^{1}H NMR (500 MHz, Chloroform-*d*) δ 7.67 (d, *J* = 8.9 Hz, 1H), 6.85 (dd, *J* = 8.8, 2.6 Hz, 1H), 6.82 (d, *J* = 2.5 Hz, 1H), 6.45 (s, 1H), 4.12 (s, 2H), 3.87 (s, 5H), 3.57 (s, 3H), 3.31 (s, 3H), 3.19 (s, 7H), 3.00 (d, *J* = 5.3 Hz, 4H), 1.49 (s, 9H), 1.40 (s, 18H). ^{13}C NMR (126 MHz, $CDCl_3$) δ 173.69, 172.79, 163.03, 160.59, 155.62, 152.54, 125.59, 112.81, 112.59, 111.79, 101.49, 101.21, 83.33, 82.62, 56.74, 55.92, 55.85, 55.33, 54.46, 51.76, 51.40, 28.38, 28.34, 28.22, 28.19, 28.10, 28.03.

1-(7-methoxy-4-methyl-coumarin)-4-7-10-tris(carboxylmethyl)-1,4,7,10-tetraazacyclododacane (L). Preligand **1** (586 mg, 0.83 mmol) was dissolved in dichloromethane (10 ml), trifluoroacetic acid (10 ml) was then added to the mixture. The reaction mixture was left to stir for 48 hours at room temperature. The solvent was removed under reduced pressure and the residue dissolved in the minimum amount of methanol and precipitated with diethyl ether. Trituration with diethyl ether yielded the product as a slightly yellow solid in quantitative yield. ESI-MS: m/z calculated for $C_{25}H_{34}N_4O_9$ $[M+H]^+$ 535.2398, found 535.23987. ^{1}H NMR (500 MHz, Deuterium Oxide) δ 7.93 (d, *J* = 8.8 Hz, 1H), 7.05 – 6.98 (m, 2H), 6.65 (s, 1H), 4.12 (s, 2H), 3.94 – 3.91 (m, 3H), 3.86 (d, *J* = 16.8 Hz, 2H), 3.64 – 3.36 (m, 13H), 3.09 (dd, *J* = 58.6, 28.0 Hz, 10H).

UV/VIS spectroscopy. All spectra were recorded on a Varian Cary 6000i double beam absorption spectrophotometer, using quartz cells of 1 cm path length for Eu.**L** and 0.1 cm for Tb.**L**, Cm.**L**. All absorbance values were corrected from the absorbance of the corresponding buffer. All spectra are available in the ESI Figures S9, S13, and S17.

Luminescence spectroscopy. All steady state, excitation and emission spectra were recorded on a HORIBA Jobin Yvon IBH FluoroLog-3 spectrofluorimeter. A sub-microsecond Xenon flashlamp (Jobin Yvon, 5000XeF) was used as the light source, with an input pulse energy (100 nF discharge capacitance) of ca. 50 mJ, yielding an optical pulse duration of less than 300 ns at full width at half maximum (FWHM). Spectral selection was achieved by passage through a double grating excitation monochromator (2.1 nm/mm dispersion, 1200 grooves/mm). Emission was monitored perpendicular to the excitation pulse; again with spectral selection. The time-gated emission spectrum of Tb.**L** was recorded on a Cary Eclipse fluorescence spectrometer with a photomultiplier tube from Agilent Technologies. For all luminescence measurements, the absorbance at the excitation wavelength and longer wavelengths was kept below 0.1 to avoid inner filter effects and intermolecular interactions. All luminescence experiments were performed in either 1 cm or 0.1 cm quartz cells. Luminescence lifetimes were determined on a HORIBA Jobin Yvon IBH FluoroLog-3 spectrofluorimeter, adapted for time-correlated single photon counting (TCSPC) and multichannel scaling (MCS) measurements. The luminescence decays were analyzed and fitted to exponential decay functions using the Origin software package. All emission and excitation spectra and time-resolved emission decay profiles can be found in the ESI Figures S10-S12, S14-S16, S18-S20, and S21-25.

Quantum yields. Quantum yields were determined by the optically dilute method using eq. 1, where ϕ is the fluorescence quantum yield, Δ the gradient from the plot of integrated fluorescence intensity *vs* absorbance, and *n* the refractive index of the solvent. The subscripts ref and X denote reference and the sample respectively.

$$\Phi_X = \Phi_{ref}\left(\frac{\Delta_X}{\Delta_{ref}}\right)\left(\frac{n_X^2}{n_{ref}^2}\right) \quad (1)$$

For quantum yield calculations, an excitation wavelength of 325 nm was used for both the reference and sample. Quinine sulfate in 0.5 M sulfuric acid was used as the reference (ϕ_{ref} = 0.546), all data can be found in the ESI Figures S27-S30.

Spectrofluorimetric Competition Batch Titrations with EDTA or DTPA. Series of aqueous samples containing a fixed concentration of Eu.**L** (1.4 µM) and a varying amount of ligand competitor were prepared in KCl 0.1 M/HEPES buffer 10 mM. The total emission spectrum of the resulting solution was monitored following 325 nm excitation a 0.1 cm quartz cell.

Eu.**L** was challenged with 0 to 10 equivalents EDTA, and the samples were equilibrated in a thermostatic shaker 4 days at 60 °C and 3 days at 25 °C until equilibrium was reached and the luminescence intensity was stable. At the concentration used in these experiments, Eu(III) luminescence from Eu.**L** can be easily observed whereas Eu(III) luminescence from Eu.EDTA was too weak to be observed.

Eu.**L** was challenged with 0 to 500 equivalents of DTPA. All samples were equilibrated as described above. A ~5-fold decrease in the Eu(III) luminescence intensity is expected upon ligand exchange from Eu.**L** to Eu.DTPA.

No significant change in Eu(III) luminescence intensity were observed in either experiment, all data are included in the ESI Figures S30-S33.

Spectrofluorimetric Competition Batch Titrations with 3,4,3-LI-(1,2-HOPO). Series of aqueous samples containing a fixed concentration of M.**L** (1.4 µM of Eu.**L** or 1.2 µM of Tb.**L** or 0.11 µM of Cm.**L**) and a varying amount of the 3,4,3-LI(1,2-HOPO) competitor ligand was prepared in KCl 0.1 M/HEPES buffer 10 mM. The total emission spectrum of the resulting solution was monitored following 325 nm excitation a 0.1 cm quartz cell.

M.**L** was challenged with 0 to 50 equivalents of 3,4,3-LI(1,2-HOPO). All samples were equilibrated as described above. The metal centred luminescence increased upon ligand exchange from Eu.**L** to Eu.(3,4,3-LI(1,2-HOPO)), as the latter complex is the brigther of the two. Other changes spectral changes was also observed *i.e.* a slight shift of the emission bands and changes in the emission band intensity ratios were also onserved. 3,4,3-LI(1,2-HOPO) was found to be able to displace **L** in the Eu(III), Tb(III), and Cm(III) complexes and the stability constant could be determined as described below. All data are available in the ESI Figures S34-40.

Data Treatment. All thermodynamic data sets were imported into the refinement program *HypSpec* and analyzed by nonlinear least-squares refinement.[71] All equilibrium constants were defined as cumulative formation constants, β_{mlh} according to equation (2), where the metal and ligand are designed as M and L, respectively.

$$mM + lL + hH = [M_mL_lH_h]\,;\ \beta_{mlh} = \frac{[M_mL_lH_h]}{[M]^m[L]^l[H]^h} \quad (2)$$

All metal and ligand concentrations were fixed at values determined from the volume of standardized stock solutions. The refinements of the overall formation constants included literature values for the protonation constants and the metal hydrolysis products, the fits are included in the ESI Figures S41-S45. The reported values are from a minimum of two experiments.

Conflicts of interest

There are no conflicts to declare.

Acknowledgements

We thank Dr Andrew Kerridge for useful discussions. This work was supported by Knud Højgaards Fond, Oticon Fonden, Lundbeckfonden, Villum Fonden (grant#14922), Carlsbergfondet, the University of Copenhagen, and by the U.S. Department of Energy (DOE), Office of Science, Office of Basic Energy Sciences, Chemical Sciences, Geosciences, and Biosciences Division at the Lawrence Berkeley National Laboratory under Contract DE-AC02- 05CH1123 (RJA).

Notes and references

1. D. Parker, R. S. Dickins, H. Puschmann, C. Crossland and J. A. K. Howard, *Chem. Rev.*, 2002, **102**, 1977-2010.
2. J. C. Bunzli and C. Piguet, *Chem Rev*, 2002, **102**, 1897-1928.
3. P. Caravan, J. J. Ellison, T. J. McMurry and R. B. Lauffer, *Chemical Reviews*, 1999, **99**, 2293-2352.
4. J.-C. G. Bünzli, *Journal of Coordination Chemistry*, 2014, DOI: 10.1080/00958972.2014.957201, 1-45.
5. A. D. Sherry, P. Caravan and R. E. Lenkinski, *Journal of Magnetic Resonance Imaging*, 2009, **30**, 1240-1248.
6. E. G. Moore, A. P. Samuel and K. N. Raymond, *Acc Chem Res*, 2009, **42**, 542-552.
7. E. Terreno, D. D. Castelli, A. Viale and S. Aime, *Chem Rev*, 2010, **110**, 3019-3042.
8. S. Aime, M. Botta, M. Fasano and E. Terreno, *Accounts of Chemical Research*, 1999, **32**, 941-949.
9. M. C. Heffern, L. M. Matosziuk and T. J. Meade, *Chem Rev*, 2014, **114**, 4496-4539.
10. I. Hemmilä, S. Dakubu, V.-M. Mukkala, H. Siitari and T. Lövgren, *Analytical Biochemistry*, 1984, **137**, 335-343.
11. I. Hemmilá and V.-M. Mukkala, *Critical Reviews in Clinical Laboratory Sciences*, 2008, **38**, 441-519.
12. D. Geissler, L. J. Charbonniere, R. F. Ziessel, N. G. Butlin, H. G. Lohmannsroben and N. Hildebrandt, *Angewandte Chemie*, 2010, **49**, 1396-1401.
13. D. Geißler, S. Stufler, H.-G. Löhmannsröben and N. Hildebrandt, *Journal of the American Chemical Society*, 2012, **135**, 1102-1109.
14. R. G. BAUTISTA, in *Handbook on the Physics and Chemistry of Rare Earths*, eds. J. K.A. Gschneidner and L. Eyring, Elsevier Science 1995, vol. 21.
15. K. L. Nash and M. P. Jensen, in *Handbook on the Physics and Chemistry of Rare Earths*, eds. K. A. G. Jr and L. Eyring, Elsevier Science B V, 2000 vol. 28.
16. P. Frohlich, T. Lorenz, G. Martin, B. Brett and M. Bertau, *Angewandte Chemie*, 2017, **56**, 2544-2580.
17. W. D. Horrocks and D. R. Sudnick, *Journal of the American Chemical Society*, 1979, **101**, 334-340.
18. A. Beeby, I. M. Clarkson, R. S. Dickins, S. Faulkner, D. Parker, L. Royle, A. S. de Sousa, J. A. G. Williams and M. Woods, *Journal of the Chemical Society, Perkin Transactions 2*, 1999, DOI: 10.1039/a808692c, 493-504.
19. M. Tropiano, O. A. Blackburn, J. A. Tilney, L. R. Hill, T. Just Sørensen and S. Faulkner, *Journal of Luminescence*, 2015, **167**, 296-304.

20. I. Billard, in *Handbook on the Physics and Chemistry of Rare Earths*, eds. K. A. G. Jr, J.-C. G. Bünzli and V. K. Pecharsky, 2003, vol. 33, pp. 465-514.
21. T. J. Sørensen, A. M. Kenwright and S. Faulkner, *Chemical Science*, 2015, **6**, 2054-2059.
22. T. J. Sørensen, M. Tropiano, A. M. Kenwright and S. Faulkner, *European Journal of Inorganic Chemistry*, 2017, **2017**, 2165-2172.
23. J. Andres and K. E. Borbas, *Inorganic chemistry*, 2015, **54**, 8174-8176.
24. E. Pershagen and K. E. Borbas, *Angewandte Chemie*, 2015, **54**, 1787-1790.
25. D. Kovacs, X. Lu, L. S. Meszaros, M. Ott, J. Andres and K. E. Borbas, *Journal of the American Chemical Society*, 2017, **139**, 5756-5767.
26. M. Tropiano, O. A. Blackburn, J. A. Tilney, L. R. Hill, M. P. Placidi, R. J. Aarons, D. Sykes, M. W. Jones, A. M. Kenwright, J. S. Snaith, T. J. Sørensen and S. Faulkner, *Chem Eur J*, 2013, **19**, 16566-16571.
27. T. J. Sørensen, L. R. Hill, J. A. Tilney, O. A. Blackburn, M. W. Jones, M. Tropiano and S. Faulkner, *European Journal of Inorganic Chemistry*, 2014, **2014**, 2520-2528.
28. T. J. Sørensen, L. R. Hill and S. Faulkner, *ChemistryOpen*, 2015, **4**, 509 – 515.
29. A. M. Funk, K. L. N. A. Finney, P. Harvey, A. M. Kenwright, E. R. Neil, N. J. Rogers, P. K. Senanayake and D. Parker, *Chemical Science*, 2015, **6**, 1655-1662.
30. O. A. Blackburn, R. M. Edkins, S. Faulkner, A. M. Kenwright, D. Parker, N. J. Rogers and S. Shuvaev, *Dalton transactions*, 2016, DOI: 10.1039/C6DT00227G.
31. O. A. Blackburn, A. M. Kenwright, A. R. Jupp, J. M. Goicoechea, P. D. Beer and S. Faulkner, *Chemistry – A European Journal*, 2016, **22**, 8929 – 8936.
32. O. A. Blackburn, J. D. Routledge, L. B. Jennings, N. H. Rees, A. M. Kenwright, P. D. Beer and S. Faulkner, *Dalton transactions*, 2016, **45**, 3070-3077.
33. S. Aime, M. Botta, Z. Garda, B. E. Kucera, G. Tircso, V. G. Young and M. Woods, *Inorganic chemistry*, 2011, **50**, 7955-7965.
34. S. Aime, M. Botta and G. Ermondi, *Inorg. Chem*, 1992, **31**, 4291-4299.
35. J. F. Desreux, *Inorganic chemistry*, 1980, **19**, 1319-1324.
36. D. Lundberg and I. Persson, *Coordination Chemistry Reviews*, 2016, **318**, 131-134.
37. B. E. Allred, P. B. Rupert, S. S. Gauny, D. D. An, C. Y. Ralston, M. Sturzbecher-Hoehne, R. K. Strong and R. J. Abergel, *Proceedings of the National Academy of Sciences of the United States of America*, 2015, **112**, 10342-10347.
38. M. A. Silver, S. K. Cary, J. A. Johnson, R. E. Baumbach, A. A. Arico, M. Luckey, M. Urban, J. C. Wang, M. J. Polinski, A. Chemey, G. Liu, K.-W. Chen, S. M. Van Cleve, M. L. Marsh, T. M. Eaton, L. J. van de Burgt, A. L. Gray, D. E. Hobart, K. Hanson, L. Maron, F. Gendron, J. Autschbach, M. Speldrich, P. Kögerler, P. Yang, J. Braley and T. E. Albrecht-Schmitt, *Science*, 2016, **353**.
39. S. K. Cary, M. A. Silver, G. Liu, J. C. Wang, J. A. Bogart, J. T. Stritzinger, A. A. Arico, K. Hanson, E. J. Schelter and T. E. Albrecht-Schmitt, *Inorganic chemistry*, 2015, **54**, 11399-11404.
40. G. J. P. Deblonde, M. Sturzbecher-Hoehne, P. B. Rupert, D. D. An, M.-C. Illy, C. Y. Ralston, J. Brabec, W. A. de Jong, R. K. Strong and R. J. Abergel, *Nature Chemistry*, 2017, DOI: 10.1038/nchem.2759.
41. L. S. Natrajan, *Dalton transactions*, 2012, **41**, 13167-13172.
42. P. Thakur, J. L. Conca and G. R. Choppin, *Journal of Coordination Chemistry*, 2011, **64**, 3214-3236.
43. M. Audras, L. Berthon, N. Martin, N. Zorz and P. Moisy, *Journal of Radioanalytical and Nuclear Chemistry*, 2014, DOI: 10.1007/s10967-014-3672-2.
44. R. J. Abergel and E. Ansoborlo, *Nat Chem*, 2016, **8**, 516.
45. T. Kimura, Y. Kato, H. Takeishi and G. R. Choppin, *Journal of Alloys and Compounds* 1998, **271/273** 719–722.
46. T. Stumpf, T. Fanghänel and I. Grenthe, *J. Chem. Soc., Dalton Trans.*, 2002, DOI: 10.1039/b204679b, 3799-3804.
47. P. Lindqvist-Reis, C. Apostolidis, J. Rebizant, A. Morgenstern, R. Klenze, O. Walter, T. Fanghanel and R. G. Haire, *Angew Chem Int Ed Engl*, 2007, **46**, 919-922.
48. S. Skanthakumar, M. R. Antonio, R. E. Wilson and L. Soderholm, *Inorg Chem*, 2007, **46**, 3485-3491.
49. G. Tian, N. M. Edelstein and L. Rao, *J Phys Chem A*, 2011, **115**, 1933-1938.
50. M. Sturzbecher-Hoehne, C. Goujon, G. J. Deblonde, A. B. Mason and R. J. Abergel, *Journal of the American Chemical Society*, 2013, **135**, 2676-2683.
51. M. P. Jensen, A. H. Bond, P. G. Rickert and K. L. Nash, *Journal of Nuclear Science and Technology*, 2014, **39**, 255-258.
52. K. N. Raymond and C. W. Eigenbrot, *Accounts of Chemical Research*, 1980, **13**, 276-283.
53. R. M. Diamond, K. Street and G. T. Seaborg, *Journal of the American Chemical Society*, 1954, **76**, 1461-1469.
54. M. P. Jensen and A. H. Bond, *Journal of the American Chemical Society*, 2002, **124**, 9870-9877.
55. W. T. Carnall and K. Rajnak, *The Journal of chemical physics*, 1975, **63**, 3510.
56. W. T. Carnall, G. L. Goodman, K. Rajnak and R. S. Rana, *The Journal of chemical physics*, 1989, **90**, 3443-3457.
57. C. Szijjarto, E. Pershagen, N. O. Ilchenko and K. E. Borbas, *Chem Eur J*, 2013, **19**, 3099-3109.
58. A. Dadabhoy, S. Faulkner and P. G. Sammes, *Journal of the Chemical Society, Perkin Transactions 2*, 2002, DOI: 10.1039/b104541p, 348-357.
59. R. Arppe, N. A. Kofod, A. K. R. Junker, L. G. Nielsen, E. Dallerba and T. J. Sørensen, *European Journal of Inorganic Chemistry*, DOI: 10.1002/ejic.201700720, n/a-n/a.
60. R. HARDER and S. CHABEREK, *J. Inorg. Nucl. Chem.*, 1959, **11**, 197-209.
61. Baybarz, R. D., J. Inorg. Nucl. Chem., 1965, 27, 1831-1839.
62. Fuger, J., J. Inorg. Nucl. Chem., 1958, 5, 332-338.
63. W. P. Cacheris, S. K. Nickle and A. D. Sherry, *Inorganic chemistry*, 1987, **26**, 958-960.
64. M. F. Loncin, J. F. Desreux and E. Merciny, *Inorganic chemistry*, 1986, **25**, 2646-2648.
65. S. Cotton, *Lanthanide and Actinide Chemistry*, Wiley, Chichester, 2006.
66. T. Kimura, R. Nagaishi, Y. Kato and Z. Yoshida, *Radiochim Acta*, 2001, **89**, 125-130.
67. T. Kimura and G. R. Choppin, *Journal of Alloys and Compounds*, 1994, **213**, 313-317.
68. R. J. Abergel, A. D'Aleo, C. N. Leung, D. K. Shuh and K. N. Raymond, *Inorganic chemistry*, 2009, **48**, 10868-10870.

69. M. Sturzbecher-Hoehne, C. N. Leung, A. D'Aleo, B. Kullgren, A. L. Prigent, D. K. Shuh, K. N. Raymond and R. J. Abergel, *Dalton transactions*, 2011, **40**, 8340-8346.
70. M. Sturzbecher-Hoehne, B. Kullgren, E. E. Jarvis, D. D. An and R. J. Abergel, *Chem Eur J*, 2014, **20**, 9962-9968.
71. P. Gans, A. Sabatini and A. Vacca, *Talanta*, 1996, **43**, 1739-1753.
72. A. K. R. Junker, L. R. Hill, A. L. Thompson, S. Faulkner and T. J. Sørensen, *Dalton transactions*, 2018, **47**, 4794-4803.